computation

MDPI

Article

Traveling Wave Solutions of a Four Dimensional Reaction-Diffusion Model for Porcine Reproductive and Respiratory Syndrome with Time Dependent Infection Rate

Jeerawan Suksamran [1,2,*], Yongwimon Lenbury [2,3] and Sanoe Koonprasert [1]

[1] Department of Mathematics, Faculty of Applied Science, King Mongkut's University of Technology North Bangkok, Bangkok 10800, Thailand; sanoe.k@sci.kmutnb.ac.th
[2] Centre of Excellence in Mathematics, CHE, Bangkok 10400, Thailand; scylb@yahoo.com
[3] Department of Mathematics, Faculty of Science, Mahidol University, Bangkok 10400, Thailand
* Correspondence: jeerawan.s@sci.kmutnb.ac.th

Abstract: Porcine reproductive and respiratory syndrome virus (PRRSV) causes reproductive failure in sows and respiratory disease in piglets and growing pigs. The disease rapidly spreads in swine populations, making it a serious problem causing great financial losses to the swine industry. However, past mathematical models used to describe the spread of the disease have not yielded sufficient understanding of its spatial transmission. This work has been designed to investigate a mathematical model for the spread of PRRSV considering both time and spatial dimensions as well as the observed decline in infectiousness as time progresses. Moreover, our model incorporates into the dynamics the assumption that some members of the infected population may recover from the disease and become immune. Analytical solutions are derived by using the modified extended hyperbolic tangent method with the introduction of traveling wave coordinate. We also carry out a stability and phase analysis in order to obtain a clearer understanding of how PRRSV spreads spatially through time.

Keywords: PRRSV; exponential infection rate decline; immune; stability; traveling waves; modified extended tanh function

Citation: Suksamran, J.; Lenbury, Y.; Koonprasert, S. Traveling Wave Solutions of a Four Dimensional Reaction-Diffusion Model for Porcine Reproductive and Respiratory Syndrome with Time Dependent Infection Rate. *Computation* **2021**, *9*, 30. https://doi.org/10.3390/computation9030030

Academic Editor: Gennady Bocharov

Received: 31 January 2021
Accepted: 8 March 2021
Published: 9 March 2021

1. Introduction

Porcine reproductive and respiratory syndrome (PRRS) was first reported in the United States in 1987. The causative agent of PRRS is porcine reproductive and respiratory syndrome virus (PRRSV), which was first isolated in Europe by Wensvoort et al. [1] in 1991 and then in the U.S. by Collins et al. [2]. PRRSV is classified as a member of the Arteriviridae family, Nidovirales order [3,4]. The important outcomes of the disease are severe reproductive disorders in sows, as well as respiratory problems in piglets and growing pigs. PRRSV has two genotypes—type 1 (European) and type 2 (North American) with genetic, antigenic and virulence differences having been observed to exist between American and European isolates [5]. Infected swine may recover from the disease and become immune by vaccination or innate immunity. For several decades, many researchers have carried out experiments and investigations concerning the virus to develop a PRRSV vaccine. In 2011, Sang et al. [6] studied the interaction between PRRSV and porcine innate immunity at the cellular and molecular levels. They investigated the component of the innate antiviral immune system in its response to and subversion of the infection.

In 2014, Li et al. [7] reported on their comparison between immune responses of modified live PRRSV vaccine, MLV in short, its parental strain VR-2332, and a Kansas isolate of PRRSV, namely the heterologous KS-06-72109 strain. They concluded that MLV can ensure total protection from the homologous virus VR-2332 while providing only limited protection from the heterologous KS-06 challenge.

In 2017, Yang and Zhang [8] introduced Janus kinase (JAK)-signal transducer and activator of transcription (STAT) signaling, which is activated by myriad cytokines and

involved in regulation of cell growth, proliferation, differentiation, apoptosis, angiogenesis, immunity and inflammatory response. They summarized how the PRRSV interferes with myriad cytokines and provided a perspective on the observed perturbation in the context of PRRSV-elicited immune response.

In the same year, Rahe and Murtaugh [9] investigated cellular and humoral components of the adaptive immune response, which is essential for the development of protective immunity against PRRSV. They investigated the B cell and T cell that respond to PRRSV adaptive immunity.

In 2018, Drigo et al. [10] studied the time-course of humoral and cell-mediated components in PRRS-stable and unstable herds. They investigated the group oral fluid samples Real-time RT-PCR, PRRSV-specific IgA and IgG in oral fluids, serum IgG antibody and the cell-mediated response in whole blood samples.

In 2019, Kittiwan et al. [11] studied the humoral and cell-mediated immune responses to PRRSV that used 10 PRRSV vaccinated and 10 nonvaccinated young pigs. They used ELISA and flow cytometry analysis to determine PRRSV-specific humoral and cell-mediated immune response.

In 2019, Crisci et al. [12] studied the interactions of two enveloped RNA viruses of PRRSV and swine influenza virus (SwIV). PRRSV and SwIV are etiologic agents of porcine respiratory disease complex (PRDC) that gives rise to reduced performance and increased mortality in the porcine cellular innate immunity during infection.

In the same year, Phoo-ngurn et al. [13] introduced a dynamical model for the progression of PRRSV and the impact of immunity information, subject to various control policies that include vaccinating. They explored the effects of two vaccination strategies, namely vaccination at the moment of birth and vaccinating those selected from a pool of susceptibles.

In 2020, Madapong et al. [14] investigated cell-mediated immunity (CMI), IL-10, and the protective efficacy of modified-live porcine reproductive and respiratory syndrome virus (PRRSV) vaccines (MLV) against co-challenge with PRRSV-1 and PRRSV-2 (HP-PRRSV). They divided pigs into seven groups, six of which were intramuscularly vaccinated with MLV, including Porcilis (PRRSV-1 MLV, MSD Animal Health, Boxmeer, The Netherlands), Amervac (PRRSV-1 MLV, Laboratorios Hipra, Girona, Spain), Fostera (PRRSV-2 MLV, Zoetis Inc., Troy Hills, U.S.), Ingelvac PRRS MLV and Ingelvac PRRS ATP (PRRSV-2, Boehringer Ingelheim, Rhein, Germany), Prime Pac PRRS (PRRSV-2 MLV, MSD Animal Health, Boxmeer, The Netherlands) and one of which was unvaccinated.

These infectious diseases in swine farms lead to financial losses in pork industries and place a heavy burden on the countries' economy. Mathematical modeling is an important tool to describe the behavior of the disease and efficiency of control strategies. In this paper, we investigate a mathematical model, proposed in the next section, for the spread of PRRSV that incorporates both time and spatial dimensions as well as the observed decline in infectiousness as time progresses. Moreover, our model incorporates into the dynamics the assumption some members of the infected population may recover from the disease and become immune. In Section 3, the model is also analyzed for its stability, assisted by a phase analysis that allows us to obtain a clearer understanding of how PRRSV spreads spatially through time. We then derive, in Section 4, the analytical solution of the model by introducing a new coordinate known as the traveling wave coordinate and applying the modified extended hyperbolic tangent method [15–21]. Concluding remarks are given in the last section.

2. Materials and Methods

Here, we consider a system of reaction-diffusion equations to describe the spread of populations in space and assume that the population has a size N over the period of the epidemic.

In 2017, Suksamran et al. [22] presented a model that considers the dimensions of both time and space in the progression of PRRSV and that also pays attention to the how the disease's infectiousness declines as time passes, as follows:

$$\frac{\partial S}{\partial t} = \frac{\partial^2 S}{\partial x^2} + b_S S + b_{SI} I - d_S S - \beta S G, \tag{1}$$

$$\frac{\partial I}{\partial t} = \beta S G + b_I I - d_I I, \tag{2}$$

$$\frac{\partial G}{\partial t} = \alpha I - \gamma G, \tag{3}$$

where $S(x,t)$ is the number per unit area of the susceptible swine at time t, measured in days, and spatial distance x, and $I(x,t)$ is the number per unit area of the infected swine at time t and spatial distance x. The first term on the right of (1) is the rate that $S(x,t)$ spreads as a diffusive process in space. The second and third terms here are the birth rates of susceptible populations arising from the susceptible and infected pools, respectively. The last term in (1) represents the rate that $S(x,t)$ is removed due to infection.

In [22], the authors denoted by G the integral expression that represents the rate of at which susceptible swine becomes infected, written as

$$G = \int_0^t \alpha e^{-\gamma(t-\tau)} I(x,\tau) d\tau, \tag{4}$$

which declines with time. This term has been introduced into the 3-dimensional model considered in [22]. It accounts for the decline in infectiousness of diseased swine with time, which is a characteristic specific to the virus of interest, namely the PRRSV. This pattern of infection rate was pointed out in the work of Charpin et al. in [23], which reported on the data collected from the swine population infected with PRRSV. The graph of (4), shown in [22], has the same shape qualitatively as that plotted from experimental data in [23]. The values of the parameters α and γ are specific to the infected population of interest and should be fitted with observed data when the result of this study is to be used in the field.

Equation (2) gives the rate of change of the infected population, in which the first term is the rate of its increase due to infection of $S(x,t)$ when coming in contact with $I(x,t)$. The last two terms here are, respectively, the birth and death rates of $I(x,t)$. The rate of change of G can be written as in (3), obtained from simply differentiating G with time, with α and γ being constants of variation in the integral function G. Please see [22] for more detail.

The system parameters in the referenced models discussed in this and later sections are defined in Table 1.

Table 1. List of parameters in porcine reproductive and respiratory syndrome virus (PRRSV) model and their definitions.

Parameter	Description
b_S	Specific birth rate of susceptible population from susceptible population
b_{SI}	Specific birth rate of susceptible population from infected population
d_S	Specific death rate of susceptible population
β	Transmission coefficient
ρ	Removal rate of recovered population
b_I	Specific birth rate of infection population
d_I	Specific death rate of infection population
η	Specific recovery rate of infected population
d_R	Specific death rate of recovered population
α	Constant of variation in the rate equation for G
γ	Rate of increase in G per unit of I

We would like to discover the patterns of disease distribution in the situation where infected swine could recover, or an isolation strategy is implemented in the attempt to curb the spread of the infection. We therefore modify the model (1)–(3) of PRRSV by the assumption that some members of the infected population may recover or be removed from the infected population:

$$\frac{\partial S}{\partial t} = \frac{\partial^2 S}{\partial x^2} + b_S S + b_{SI} I - d_S S - \beta SG + \rho R, \tag{5}$$

$$\frac{\partial I}{\partial t} = \beta SG + b_I I - d_I I - \eta I, \tag{6}$$

$$\frac{\partial G}{\partial t} = \alpha I - \gamma G, \tag{7}$$

$$\frac{\partial R}{\partial t} = \eta I - d_R R - \rho R, \tag{8}$$

where $R(x,t)$ is the number per unit area of the recovered or isolated swine at time t and spatial distance x. ρ is the specific rate at which $R(x,t)$ returns to the susceptible pool, η is the specific rate of decrease of infectious swine due to recovery or isolation, and d_R is the specific death rate of recovered or isolated swine.

In order to transform (5)–(8) into a system of ordinary differential equations that is easier to be analyzed, traveling wave coordinate $\xi = x - ct$, is introduced, where c is the constant speed at which the wave is assumed to be moving. By using ξ in (5)–(8), we obtain the following system of nonlinear ordinary differential equations:

$$-cs' = s'' + b_S s + b_{SI} i - d_S s - \beta sg + \rho r, \tag{9}$$

$$-ci' = \beta sg + b_I i - d_I i - \eta i, \tag{10}$$

$$-cg' = \alpha i - \gamma g, \tag{11}$$

$$-cr' = \eta i - d_R r - \rho r, \tag{12}$$

where $(\,)'$ stands for the derivative of the specific state variable with respect to ξ,$s(\xi) = S(x,t)$, $i(\xi) = I(x,t)$,$g(\xi) = G(x,t)$ and $r(\xi) = R(x,t)$.

Letting $y_1 = s$, $y_2 = s'$, $y_3 = i$, $y_4 = g$, $y_5 = r$, we can write (8)–(11) as

$$\begin{aligned}
y_1' &= y_2,\\
y_2' &= -cy_2 - b_S y_1 - b_{SI} y_3 + d_S y_1 + \beta y_1 y_4 - \rho y_5,\\
y_3' &= -\tfrac{\beta}{c} y_1 y_4 - \tfrac{b_I}{c} y_3 + \tfrac{d_I}{c} y_3 + \tfrac{\eta}{c} y_3,\\
y_4' &= -\tfrac{\alpha}{c} y_3 + \tfrac{\gamma}{c} y_4,\\
y_5' &= -\tfrac{\eta}{c} y_3 + \tfrac{d_R}{c} y_5 + \tfrac{\rho}{c} y_5.
\end{aligned} \tag{13}$$

Next, we shall analyze the model system (12) for its stability.

3. Model Analysis

Here, we carry out a stability analysis of the system (13) that results from the transformation of (5)–(8). Two steady state solutions can be directly found for the system (13), namely $E_0 = (0,0,0,0,0)$ and $E_1 = \left(\frac{(d_I - b_I + \eta)\gamma}{\alpha\beta}, 0, \frac{\gamma\kappa}{\alpha}, \kappa, \frac{\eta\gamma\kappa}{\alpha(d_R+\rho)}\right)$, where $\kappa = \frac{(d_S - b_S)(d_I - b_I + \eta)(d_R + \rho)}{\beta[(d_R+\rho)(b_{SI} - d_I + b_I - \eta) + \rho\eta]}$. We note that the equilibrium point E_1 exists only if

$$d_S - b_S > 0 \tag{14}$$

and

$$\frac{d_I - b_I + \eta}{c^2} > 1, \tag{15}$$

in which case the denominator of κ will be positive, and all components of E_1 will be positive as well.

The Jacobian matrix of the system (13) evaluated at an arbitrary steady state $\left(y_1^*, y_2^*, y_3^*, y_4^*, y_5^*\right)$ is

$$\overline{J} = \begin{pmatrix} 0 & 1 & 0 & 0 & 0 \\ d_S - b_S + \beta y_4^* & -c & -b_{SI} & \beta y_1^* & -\rho \\ -\frac{\beta}{c} y_4^* & 0 & \frac{d_I - b_I + \eta}{c} & -\frac{\beta}{c} y_1^* & 0 \\ 0 & 0 & -\frac{\alpha}{c} & \frac{\gamma}{c} & 0 \\ 0 & 0 & -\frac{\eta}{c} & 0 & \frac{d_R + \rho}{c} \end{pmatrix}.$$

At the washout steady state $E_0 = (0, 0, 0, 0, 0)$, the Jacobian matrix can be written as

$$\overline{J}_0 = \begin{pmatrix} 0 & 1 & 0 & 0 & 0 \\ d_S - b_S & -c & -b_{SI} & 0 & -\rho \\ 0 & 0 & \frac{d_I - b_I + \eta}{c} & 0 & 0 \\ 0 & 0 & -\frac{\alpha}{c} & \frac{\gamma}{c} & 0 \\ 0 & 0 & -\frac{\eta}{c} & 0 & \frac{d_R + \rho}{c} \end{pmatrix},$$

whose eigenvalues are

$$\lambda_1 = \frac{d_I - b_I + \eta}{c},$$

$$\lambda_2 = \frac{\gamma}{c},$$

$$\lambda_3 = \frac{d_R + \rho}{c}$$

and

$$\lambda_{4,5} = \frac{-c \pm \sqrt{c^2 - 4(b_S - d_S)}}{2}.$$

Since λ_2 and λ_3 are positive, this equilibrium point is unstable. Since, by (14), $d_S - b_S > 0$, or by (15) we have $d_I - b_I + \eta < 0$, it can be concluded that E_0 is a saddle point.

Theorem 1. *The equilibrium solution $E_1 = \left(y_1^*, y_2^*, y_3^*, y_4^*, y_5^*\right)$ of (13) is unstable for all positive parameter values whenever it exists.*

Proof of Theorem 1. We calculate the Jacobian matrix of the system (13) at E_1 to obtain

$$\overline{J}_1 = \begin{pmatrix} 0 & 1 & 0 & 0 & 0 \\ d_S - b_S + \beta y_4^* & -c & -b_{SI} & \beta y_1^* & -\rho \\ -\frac{\beta}{c} y_4^* & 0 & \frac{\eta + d_I - b_I}{c} & -\frac{\beta}{c} y_1^* & 0 \\ 0 & 0 & -\frac{\alpha}{c} & \frac{\gamma}{c} & 0 \\ 0 & 0 & -\frac{\eta}{c} & 0 & \frac{d_R + \rho}{c} \end{pmatrix},$$

whose characteristic equation is

$$\lambda^5 + A_1\lambda^4 + A_2\lambda^3 + A_3\lambda^2 + A_4\lambda + A_5 = 0,$$

where $A_1 = c - \frac{d_I + d_R - b_I + \gamma + \eta + \rho}{c}$,

$$A_2 = b_S + b_I - d_S - d_I - d_R - \beta\kappa - \gamma - \eta - \rho + \frac{(d_R + \rho)(d_I - b_I + \gamma + \eta)}{c^2},$$

$$A_3 = \begin{array}{l} \frac{\beta\kappa(d_I + d_R - b_I - b_{SI} + \gamma + \eta + \rho) + \rho(d_S + d_I - b_S - b_I + \gamma + \eta)}{c} \\ + \frac{(b_S - d_S - d_R)(b_I - \gamma - \eta) + (d_I + d_R)(d_S - b_S) + d_I d_R}{c}, \end{array} \quad (16)$$

$$A_4 = \frac{\beta\kappa[\gamma(b_I+b_{SI}-d_I-d_R-\rho)-\eta(d_R+\gamma)+(d_R+\rho)(b_I+b_{SI}-d_I)]}{c^2} + \frac{(b_S-d_S)(d_R+\rho)(d_I-b_I+\gamma+\eta)}{c^2},$$

$$A_5 = \frac{\beta\gamma\kappa[(d_I-b_I-b_{SI})(d_R+\rho)+\eta d_R]}{c^2}.$$

According to the Routh–Hurwitz stability criterion [24], the solution of E_1 will be stable when the coefficients in the characteristic equation are all positive. However, the coefficient of λ^4 is

$$c - \frac{d_I + d_R - b_I + \gamma + \eta + \rho}{c} < 0,$$

since (14) and (15) must hold for this equilibrium point E_1 to exist. So that this equilibrium solution E_1 is unstable whenever it exists. This ends the proof. □

Figure 1 shows the phase portrait in the (y_1, y_2)-plane. Here, we see that the solution trajectories diverge, as expected, from the origin, which is a saddle point as theoretically predicted in Theorem 1. The parametric values used in the plot in Figure 1 have been chosen to satisfy the required inequalities (14)–(15) and the equations in (16), as given in Table 2.

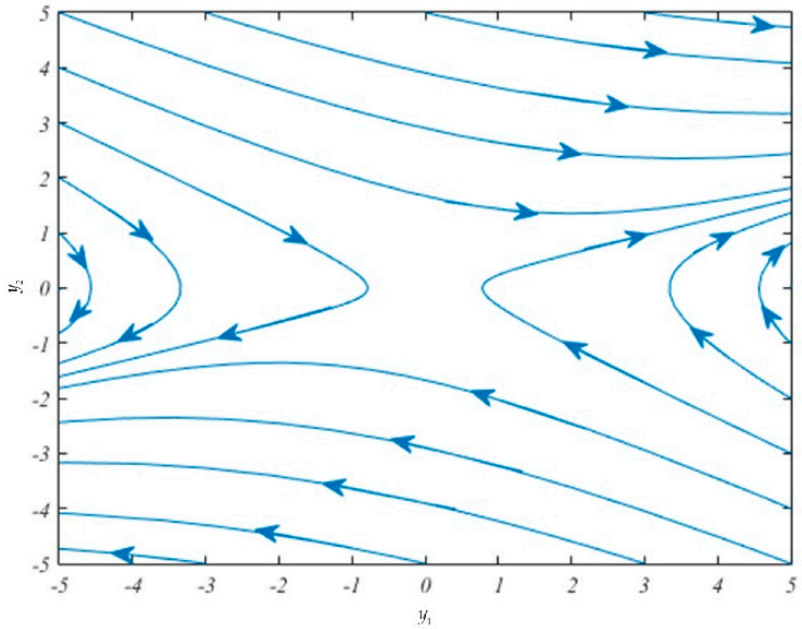

Figure 1. Plot of the phase portrait, in the (y_1, y_2)-plane, of the model system (13).

Table 2. List of parametric values for PRRSV model system (13).

Parameter	Value	Unit
b_S	0.6	day^{-1}
b_{SI}	0.6	day^{-1}
d_S	0.8	day^{-1}
β	0.5	day^{-1}
ρ	0.3	day^{-1}
b_I	0.4	day^{-1}
d_I	0.3	day^{-1}
η	0.2	day^{-1}
d_R	0.2	day^{-1}
α	0.4	day^{-1} per swine
γ	0.5	day^{-1}

In the next section, we derive analytical solutions for our system model (5)–(8).

The novel insights into the dynamics of PRRS provided by the above analysis may be implied from the above theorem, which states that the equilibrium points of the model system are both unstable, which means that it will not be possible for us to control the infection to remain at a steady level, even though some of the infected swine can recover or are put in isolation. Other more effective control policies should be adopted in order to mitigate the situation, such as vaccination or culling. This could be the subject for future studies.

4. Analytical Solution

In this section, we apply the modified extended tanh method [15–21] to derive analytical solutions in term traveling wave coordinate. For the readers who may not be familiar with the method, a brief summary of the modified extended tanh method is provided in Appendix A. Accordingly, the solution of the model Equations (9)–(12) can be expressed as finite series of tanh functions in the following form

$$s(\xi) = \sum_{m=0}^{M} a_m \phi^m, \tag{17}$$

$$i(\xi) = \sum_{n=0}^{N} b_n \phi^n, \tag{18}$$

$$g(\xi) = \sum_{p=0}^{P} c_p \phi^p, \tag{19}$$

$$r(\xi) = \sum_{q=0}^{Q} d_q \phi^q, \tag{20}$$

where a_m, b_n, c_p and d_q are constants, and $\phi(\xi) = \tanh(\mu\xi)$ satisfy the Riccati equation

$$\phi' = \mu\left(1 - \phi^2\right).$$

The values of M, N, P and Q are determined by equating the highest order of ϕ in the nonlinear expression sg with the highest order of ϕ in the linear expression s'' in (9) yielding

$$M + 2 = M + P,$$

therefore $P = 2$. Equating the highest order of ϕ in the nonlinear expression sg with the highest order of ϕ in the linear expression i' in (10) yields

$$N + 1 = M + P = M + 2,$$

therefore $N = M + 1$, Equating the highest order of ϕ in the expression i with the highest order of ϕ in the linear expression g' in (11) yields

$$P + 1 = N,$$

so that $N = 3$. Equating the highest order of ϕ in the expression i with the highest order of ϕ in the linear expression r' in (12) gives

$$Q + 1 = N.$$

Thus, we have found that

$$M = 2,\ N = 3,\ P = 2 \text{ and } Q = 2. \tag{21}$$

If we substitute (21) into (17)–(20), we will arrive at

$$s(\xi) = a_0 + a_1\phi + a_2\phi^2, \tag{22}$$

$$i(\xi) = b_0 + b_1\phi + b_2\phi^2 + b_3\phi^3, \tag{23}$$

$$g(\xi) = c_0 + c_1\phi + c_2\phi^2, \tag{24}$$

$$r(\xi) = d_0 + d_1\phi + d_2\phi^2. \tag{25}$$

Substituting $\phi(\xi) = \tanh(\mu\xi)$ and the Riccati equation in Equations (9)–(12), with the assistance of (22)–(25), and equating the coefficients of terms of equal powers of ϕ, we arrive at the following system of algebraic equations that govern the parameters $a_0, a_1, a_2, b_0, b_1, b_2, b_3, c_0, c_1, c_2, d_0, d_1, d_2$:

$$\begin{gathered}
ca_1\mu + 2a_2\mu^2 + b_S a_0 + b_{SI} b_0 - d_S a_0 + \rho d_0 - \beta a_0 c_0 = 0,\\
2ca_2\mu - 2a_1\mu^2 + b_S a_1 + b_{SI} b_1 - d_S a_1 + \rho d_1 - \beta a_0 c_1 - \beta a_1 c_0 = 0,\\
b_S a_2 + b_{SI} b_2 - d_S a_2 - ca_1\mu - 8a_2\mu^2 + \rho d_2 - \beta a_0 c_2 - \beta a_1 c_1 - \beta a_2 c_0 = 0,\\
2a_1\mu^2 - 2ca_2\mu + b_{SI} b_3 - \beta a_1 c_2 - \beta a_2 c_1 = 0,\\
6a_2\mu^2 - \beta a_2 c_2 = 0,\\
cb_1\mu + b_I b_0 - d_I b_0 - \eta b_0 + \beta a_0 c_0 = 0,\\
2cb_2\mu + b_I b_1 - d_I b_1 - \eta b_1 + \beta a_0 c_1 + \beta a_1 c_0 = 0,\\
3cb_3\mu - cb_1\mu + b_I b_2 - d_I b_2 - \eta b_2 + \beta a_0 c_2 + \beta a_1 c_1 + \beta a_2 c_0 = 0,\\
b_I b_3 - 2cb_2\mu - d_I b_3 - \eta b_3 + \beta a_1 c_2 + \beta a_2 c_1 = 0,\\
\beta a_2 c_2 - 3cb_3\mu = 0,\ cc_1\mu + \alpha b_0 - \gamma c_0 = 0,\\
2cc_2\mu + \alpha b_1 - \gamma c_1 = 0,\ \alpha b_2 - \gamma c_2 - cc_1\mu = 0,\\
\alpha b_3 - 2cc_2\mu = 0,\\
cd_1\mu - d_R d_0 + \eta b_0 - \rho d_0 = 0,\\
2cd_2\mu + \eta b_1 - d_R d_1 - \rho d_1 = 0,\\
\eta b_2 - cd_1\mu - d_R d_2 - \rho d_2 = 0,\\
\eta b_3 - 2cd_2\mu = 0
\end{gathered} \tag{26}$$

Solving the system (26), we obtain the parameters $a_0, a_1, a_2, b_0, b_1, b_2, b_3, c_0, c_1, c_2, d_1, d_2$ expressed in term d_0 as follows:

$$\begin{gathered}
a_0 = \left[\frac{6\mu^2}{\alpha\beta} + \frac{d_0}{\eta}\right]\frac{(d_R+\rho)(d_I+\eta-b_{SI}-b_I)}{(b_S-d_S)} - \left[\frac{6\eta\mu^2}{\alpha\beta} + d_0\right]\frac{\rho}{(b_S-d_S)} - \frac{6c^2\mu^2}{\alpha\beta},\\
a_1 = \frac{6c\mu\left(d_R+\rho+\gamma+b_{SI}+b_I-d_I-\eta+c^2\right)}{\alpha\beta},\ a_2 = \frac{6c^2\mu^2}{\alpha\beta},\\
b_0 = \frac{d_0(d_R+\rho)}{\eta} - \frac{6\gamma\mu^2}{\alpha\beta},\ b_1 = \frac{6\gamma\mu(d_R+\rho)}{c\alpha\beta} - \frac{12c\mu^3}{\alpha\beta},\ b_2 = \frac{6\mu^2(d_R+\rho+\gamma)}{\alpha\beta},\ b_3 = \frac{12c\mu^3}{\alpha\beta},\\
c_0 = \frac{\alpha d_0(d_R+\rho)}{\gamma\eta} - \frac{6\mu^2(d_R+\rho-\gamma)}{\gamma\beta},\ c_1 = \frac{6\mu(d_R+\rho)}{c\beta},\ c_2 = \frac{6\mu^2}{\beta},\\
d_1 = \frac{6\gamma\eta\mu}{c\alpha\beta},\ d_2 = \frac{6\eta\mu^2}{\alpha\beta}.
\end{gathered} \tag{27}$$

Thus, the exact solution of the model system can be written as follows:

$$\begin{aligned} S(x,t) = {} & \left[\frac{6\mu^2}{\alpha\beta} + \frac{d_0}{\eta}\right]\frac{(d_R+\rho)(d_I+\eta-b_{SI}-b_I)}{(b_S-d_S)} - \left[\frac{6\eta\mu^2}{\alpha\beta} + d_0\right]\frac{\rho}{(b_S-d_S)} - \frac{6c^2\mu^2}{\alpha\beta} \\ & + \frac{6c\mu\left(d_R+\rho+\gamma+b_{SI}+b_I-d_I-\eta+c^2\right)}{\alpha\beta}\tanh(\mu(x-ct)) \\ & + \frac{6c^2\mu^2}{\alpha\beta}\tanh^2(\mu(x-ct)), \end{aligned} \tag{28}$$

$$\begin{aligned} I(x,t) = {} & \frac{d_0(d_R+\rho)}{\eta} - \frac{6\gamma\mu^2}{\alpha\beta} + \left[\frac{6\gamma\mu(d_R+\rho)}{c\alpha\beta} - \frac{12c\mu^3}{\alpha\beta}\right]\tanh(\mu(x-ct)) \\ & + \frac{6\mu^2(d_R+\rho+\gamma)}{\alpha\beta}\tanh^2(\mu(x-ct)) + \frac{12c\mu^3}{\alpha\beta}\tanh^3(\mu(x-ct)), \end{aligned} \tag{29}$$

$$\begin{aligned} G(x,t) = {} & \left[\frac{6\mu^2(d_R+\rho-\gamma)}{\gamma\beta} + \frac{\alpha d_0(d_R+\rho)}{\gamma\eta}\right] + \frac{6\mu(d_R+\rho)}{c\beta}\tanh(\mu(x-ct)) \\ & + \frac{6\mu^2}{\beta}\tanh^2(\mu(x-ct)), \end{aligned} \tag{30}$$

$$R(x,t) = d_0 + \frac{6\gamma\eta\mu}{c\alpha\beta}\tanh(\mu(x-ct)) + \frac{6\eta\mu^2}{\alpha\beta}\tanh^2(\mu(x-ct)). \tag{31}$$

Figure 2 shows the plots of the wave fronts of the susceptible population $S(x,t)$ in Figure 2a, the infected population $I(x,t)$ in Figure 2b, and the recovered population $R(x,t)$ in Figure 2c, given in (28), (29) and (31), respectively. Here $a_0 = 1.1345$, $a_1 = 0.5355$, $a_2 = 0.00675$, $b_0 = 0.9625$, $b_1 = 1.24775$, $b_2 = 0.075$, $b_3 = 0.00225$, $c_0 = 0.8$, $c_1 = 1$, $c_2 = 0.03$, $d_0 = 0.4$, $d_1 = 0.5$, and $d_2 = 0.015$. All parametric values have been chosen to satisfy inequalities (14)–(15) as well as Equations (15) and (26). We show the plots of proportions of susceptible, the infected and the recovered swine given by Equations (28), (29) and (31) as functions of radial distance x. The waves travel from left to right as time passes.

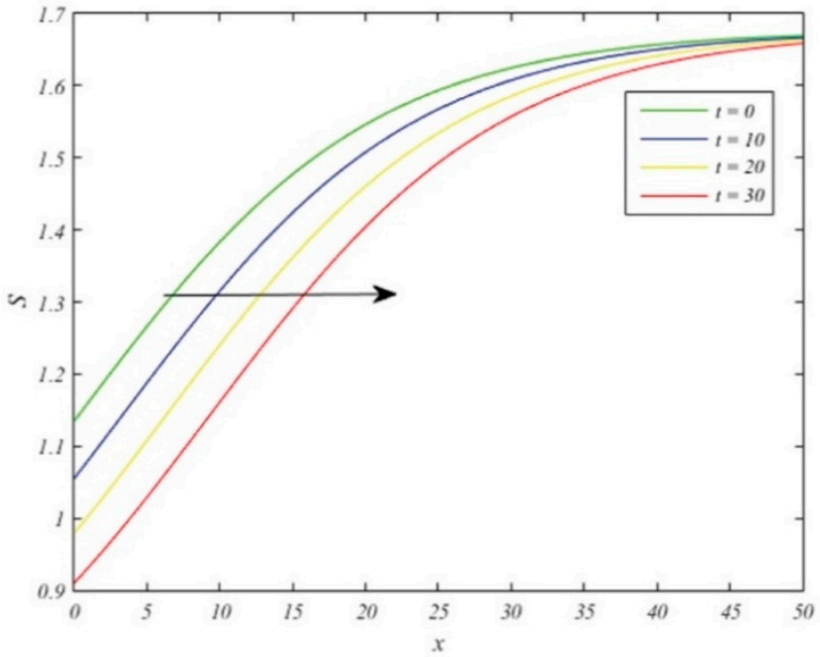

(**a**)

Figure 2. *Cont.*

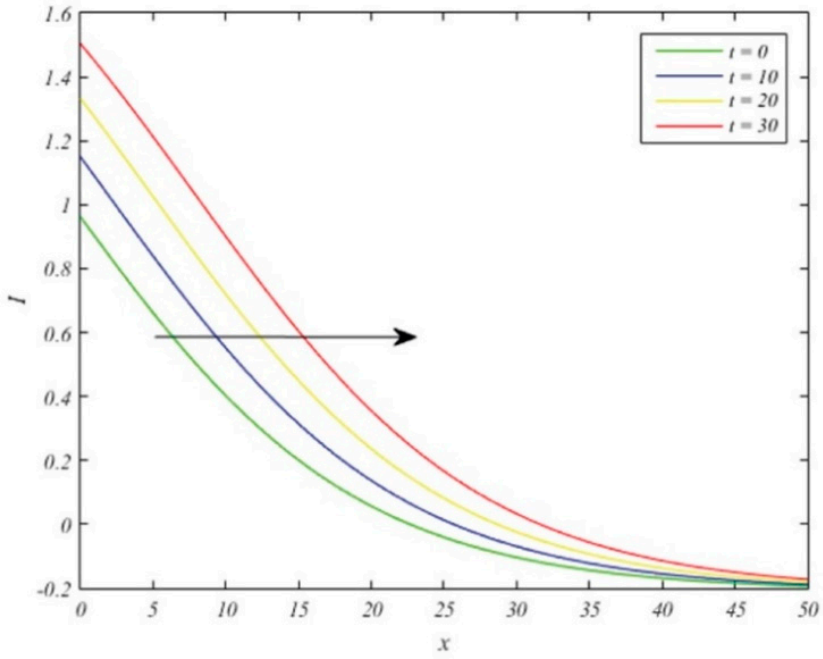

(**b**)

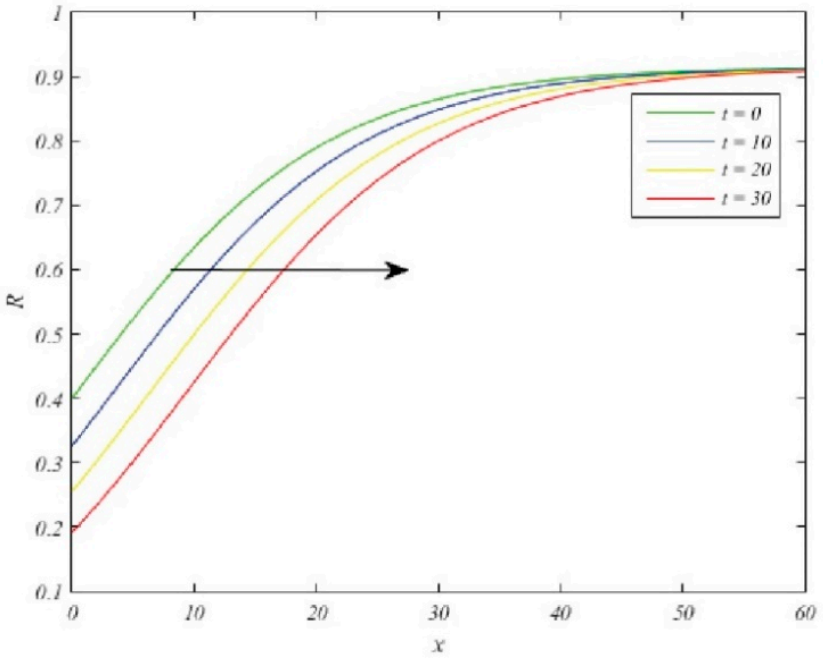

(**c**)

Figure 2. Traveling wave solution: (**a**) susceptible population per unit area; (**b**) infected population per unit area; (**c**) recovered population per unit area. The waves are plotted as functions of x for t between 0 (left most) and 30 (right most). Here, $S(0,0) = 1.1345$, $I(0,0) = 0.9625$, $G(0,0) = 0.8$, $R(0,0) = 0.4$, and other parameter values are as given in the text.

The plots of wave fronts shown in Figure 2 contribute to our understanding of the manner in which the infection spreads through space and time. They depict the situation in which the infection starts out not being that widespread at the central point of the region of interest where $x = 0$, while some pigs remain healthy here. As time progresses, the

number of infected swine incidences at this point increases, while the counts of susceptible swine and the recovered swine decrease at this particular spatial location. In other words, if the location x is fixed, we can forecast the manner in which the level of the infectives will increases, while in contrast the numbers of susceptible and recovered will decrease.

On the other hand, if we remain fixed in time, but follow a single (constant-time) wave front as x increases, moving farther and farther away from the central location of the infection, we will observe that the numbers of the susceptible swine and the recovered swine farther away from the center get higher per unit area due to the fact that the infection requires some time before it can spread outward and reach that distant location.

For better understanding, we construct the 3D plots in Figure 3. Here, the levels of susceptible, infective and recovered populations are given by Equations (27), (28) and (30) as functions of x and t. Relying on this graph, we can clearly discover what would happen to the swine populations involved in the distribution of this disease as we advance in the direction where both time and space increase simultaneously.

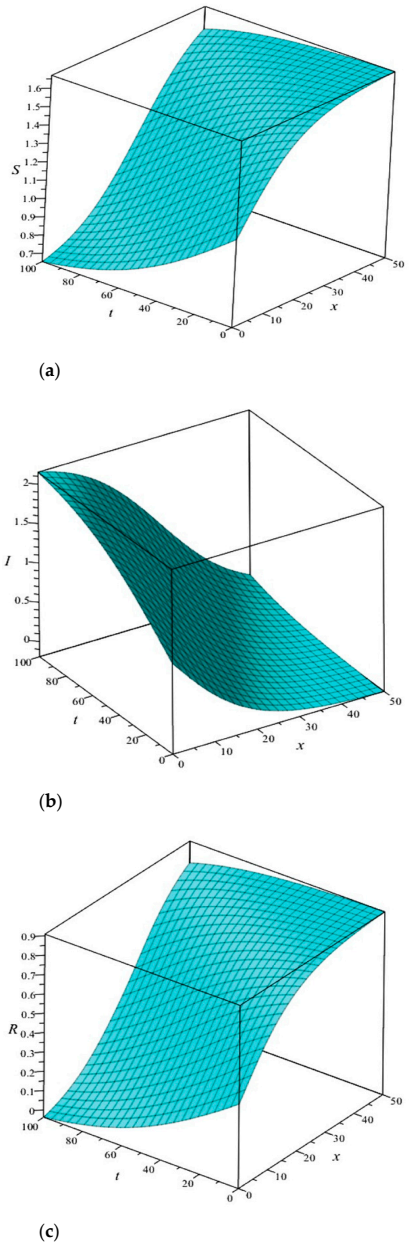

Figure 3. Three dimensional plots: (**a**) $S(x,t)$; (**b**) $I(x,t)$; (**c**) $R(x,t)$. The plots of the analytical solutions of (5)–(8) with the same set of parameters as those shown in Figure 2.

5. Conclusions

In this study, we investigated a mathematical model for the spread of PRRSV that considers both the time and spatial dimensions taking into account the reported evidence that the infectiousness declines with time subject to the assumption that some members of the infected population may recover from the disease and become immune. The stability and phase analysis of the model was carried out and interpreted, which led us to conclude that we would not be able to keep the infection under control at a steady level without application of effective control strategies. Relying on the modified extended tanh method and utilization of traveling wave coordinate, we then constructed exact traveling wave solutions to the model system. This method for finding the analytical solutions can be applied to other problems involving partial differential equations that may be transformed into systems of ordinary differential equations. Our solution provides the levels of the swine populations succumbing to PRRSV in the direction of increasing time and space.

In fact, other types of nonstationary solutions representing infection spreading (in addition to the traveling waves) could be found. According to [25], since it is difficult or often impossible to explicitly solve reaction–diffusion equations in a very general setting, researchers frequently concentrate instead on special kinds of solutions only. Especially for biological systems, we are most of the time focused on the long-term behavior, that is, what happens to the solutions a long time into the future, so that we are often led to the so-called stationary solutions. However, other types of special solutions are the so-called similarity solutions and traveling wave solutions, of which we have made use here. Solutions derived as functions of traveling wave variables are of special interest in biological sciences and medical research. They are often used to investigate invasion of species or spread of diseases in time and space, according to [25]. In our case, we have been fortunate that our model system, complicated by the integral expression, had a particularly simple form upon transformation, which allowed us to find a closed-form solution for it. Often, we will be confronted with more complicated formulas, and it will be difficult or impossible to discover a closed-form solution. In such a case, one may need to derive a numerical solution instead. Closed-form solutions are similar to numerical solutions in that their values can be found with a finite number of standard operations. However, the advantage of a closed-form solution is that it is exact, whereas a numerical solution only provides us with approximate values [26].

This method that we have adopted in trying to find the analytical solutions of our model can be applied to other problems involving partial differential equations, which may be transformed into systems of ordinary differential equations. Our solution provides the levels of the swine populations succumbing to PRRSV in the direction of increasing time and space. Specifically, if the same values have been utilized for the common set of model parameters, we would see that the level of infected swine spread out in the x direction more slowly with time when modeled with our 4-dimensional model than when the 3-dimensional model, less the recovered population, is used. Since some infected swine recover and develop immunity or are kept from infecting the susceptible swine, realistically infection would not be able to spread as quickly, which is better captured by our 4-dimensional model, which includes the rate equation for recovered population. Thus, our work has accorded us with a clearer and more comprehensive description of PRRSV progression and the possibility of reducing the rate of infection.

Author Contributions: Y.L. introduced the research problem. J.S. developed the model, assisted by Y.L., J.S. analyzed the model, assisted by S.K., and derived the analytical solution. All authors have read and agreed to the published version of the manuscript.

Funding: This research was financially supported by King Mongkut's University of Technology North Bangkok under contract no. KMUTNB-64-NEW-15.

Institutional Review Board Statement: Not applicable.

Informed Consent Statement: Not applicable.

Data Availability Statement: Not applicable.

Acknowledgments: This research project is supported in parts by the Centre of Excellence in Mathematics.

Conflicts of Interest: The authors declare no conflict of interest.

Appendix A

Modified Extended Tanh Method

Based on [15–21], we start by considering the following nonlinear partial differential equation.

$$F(u, u_t, u_x, u_{tt}, u_{xx}, \ldots) = 0, \tag{A1}$$

where F is a polynomial in $u(x,t)$ and its partial derivatives.

We seek the following traveling wave solutions:

$$u(x,t) \;=\; U(\xi), \;\; \xi \;=\; x \pm ct,$$

which are of important physical significance, where c is a constant to be determined later. Then the system (A1) reduces to a system of nonlinear ordinary differential equations (ODEs).

$$F_0\left(U, U_\xi, U_{\xi\xi}, \ldots\right) = 0, \tag{A2}$$

where F_0 is a polynomial of $U(\xi)$.

Introducing new independent variables in the form

$$Y \;=\; \tanh(\mu\xi), \quad \xi \;=\; x \pm ct, \tag{A3}$$

We are led to the change of derivatives

$$\begin{aligned}
\tfrac{d}{d\xi} &= \mu\left(1-Y^2\right)\tfrac{d}{dY},\\
\tfrac{d^2}{d\xi^2} &= -2\mu^2\left(1-Y^2\right)\tfrac{d}{dY} + \mu^2\left(1-Y^2\right)^2\tfrac{d^2}{dY^2},\\
\tfrac{d^3}{d\xi^3} &= 2\mu^3\left(1-Y^2\right)\left(3Y^2-1\right)\tfrac{d}{dY} - 6\mu^3 Y\left(1-Y^2\right)^2\tfrac{d^2}{dY^2} + \mu^3\left(1-Y^2\right)^3\tfrac{d^3}{dY^3}.
\end{aligned} \tag{A4}$$

In the context of tanh function method, many authors [15–19] used the expression

$$U(\xi) \;=\; \sum_{i=0}^{S} a_i Y^i(\xi), \tag{A5}$$

In order to construct more general solutions, it is reasonable to introduce the following expression [20,21].

$$U(\xi) \;=\; \sum_{i=0}^{S} a_i Y^i(\xi) + \sum_{i=1}^{S} b_i Y^{-i}(\xi), \tag{A6}$$

in which a_i and b_i $(i \;=\; 0, 1, \ldots, S)$ are all real constants to be determined later, the balancing number S is a positive integer which can be determined by balancing the highest order derivative terms with highest power nonlinear terms in system (A1). Substituting expression (A5) into (A2), and equating to zero the coefficients of all powers $Y^{\pm i}$ yield a set of algebraic equations for a_i, b_i, c_i, d_i and μ.

References

1. Wensvoort, G.; Terpstra, C.; Pol, J.M.A.; Laak, E.A.T.; Bloemraad, M.; Kluyver, E.P.D.; Kragten, C.; Buitten, L.V.; Besten, A.D.; Wagenaar, F.; et al. Mystery swine disease in the Netherlands: The isolation of Lelystad virus. *Vet. Q.* **1991**, *13*, 121–130. [CrossRef]
2. Collins, J.E.; Benfield, D.A.; Christianson, W.T.; Harris, L.; Hennings, J.C.; Shaw, D.P.; Goyal, S.M.; McCullough, S.; Morrison, R.B.; Joo, H.S.; et al. Isolation of swine infertility and respiratory syndrome virus (isolate ATCCVR-2332) in North America and experimental reproduction of the disease in gnotobiotic pigs. *J. Vet. Diagn. Invest.* **1992**, *4*, 117–126. [CrossRef]

3. Meulenberg, J.J.M.; Hulst, M.M.; Meijer, E.J.D.; Moonen, P.L.J.M.; Besten, A.D.; Kluyer, E.P.D.; Wensvoort, G.; Moormann, R.J.M. Lelystad virus, the causative agent of porcine epidemic abortion and respiratory syndrome (PEARS), is related to LDV and EAV. *Virology* **1993**, *192*, 62–72. [CrossRef] [PubMed]
4. Cavanaugh, D. Nidovirales: A new order comprising Coronaviridae and Arteriviridae. *Arch. Virol.* **1997**, *142*, 629–633.
5. Han, K.; Seo, H.W.; Park, C.; Oh, Y.; Kang, I.; Chae, C. Comparative pathogenesis of type 1 (European genotype) and type 2 (North American genotype) porcine reproductive and respiratory syndrome virus in infected boar. *Virol. J.* **2013**, *10*, 156. [CrossRef] [PubMed]
6. Sang, Y.; Rowland, R.R.R.; Blecha, F. Interaction between innate immunity and porcine reproductive and respiratory syndrome virus. *Anim. Health Res. Rev.* **2011**, *12*, 149–167. [CrossRef]
7. Li, X.; Galliher-Beckley, A.; Pappan, L.; Trible, B.; Kerrigan, M.; Beck, A.; Hesse, R.; Blecha, F.; Nietfeld, J.C.; Rowland, R.R.; et al. Comparison of host immune responses to homologous and heterologous type II porcine reproductive and respiratory syndrome virus (PRRSV) challenge in vaccinated and unvaccinated pigs. *Biomed Res. Int* **2014**, *2014*. [CrossRef]
8. Yang, L.; Zhang, Y.J. Antagonizing cytokine-mediated JAK-STAT signaling by porcine reproductive and respiratory syndrome virus. *Vet. Microbiol.* **2017**, *209*, 57–65. [CrossRef] [PubMed]
9. Rahe, M.C.; Murtaugh, M.P. Mechanisms of adaptive immunity to porcine reproductive and respiratory syndrome virus. *Viruses* **2017**, *9*, 148. [CrossRef] [PubMed]
10. Drigo, M.; Giacomini, E.; Lazzaro, M.; Pasotto, D.; Bilato, D.; Ruggeri, J.; Boniotti, M.B.; Alborali, G.L.; Amadori, M. Comparative evaluation of immune responses of swine in PRRS-stable and unstable herds. *Vet. Immunol. Immunopathol.* **2018**, *200*, 32–39. [CrossRef]
11. Kittiwan, N.; Yamsakul, P.; Tadee, P.; Tadee, P.; Nuangmek, A.; Chuammitri, P.; Patchanee, P. Immunological response to porcine reproductive and respiratory syndrome virus in young pigs obtained from a PRRSV-positive exposure status herd in a PRRSV endemic area. *Vet. Immunol.* **2019**, *218*, 109935. [CrossRef]
12. Crisci, E.; Fraile, L.; Montoya, M. Cellular innate immunity against PRRSV and swine influenza viruses. *Vet. Sci.* **2019**, *6*, 1–26.
13. Phoo-ngurn, P.; Kiataramkul, C.; Chamchod, F. Modeling the spread of porcine reproductive and respiratory syndrome virus (PRRSV) in a swine population: Transmission dynamics, immunity information, and optimal control strategies. *Adv. Differ. Equ.* **2019**, *432*, 1–12. [CrossRef]
14. Madapong, A.; Saeng-chuto, K.; Boonsoongnern, A.; Tantituvanont, A.; Nilubol, D. Cell-mediated immune response and protective efficacy of porcine reproductive and respiratory syndrome virus modified-live vaccines against co-challenge with PRRSV-1 and PRRSV-2. *Sci. Rep.* **2020**, *10*, 1–13. [CrossRef]
15. Malfliet, W.; Hereman, W. The Tanh Method: I. Exact solutions of nonlinear evolution and wave equations. *Phys. Scr.* **1996**, *54*, 563–568. [CrossRef]
16. Zedan, H.A. New approach for tanh and extended-tanh methods with applications on Hirota-Satsuma equations. *Comput. Appl. Math.* **2009**, *28*, 1–14.
17. Taghizadeh, N.; Mirzazadeh, M. The modified extended tanh method with the Riccati equation for solving nonlinear partial differential equations. *Math. Aeterna* **2012**, *2*, 145–153.
18. Cevikel, A.C.; Bekir, A.; Akar, M.; San, S. A procedure to construct exact solutions of nonlinear evolution equations. *J. Phys.* **2012**, *79*, 337–344. [CrossRef]
19. Malinzi, J.; Quaye, P.A. Exact solutions of non-linear evolution models in physics and biosciences using the hyperbolic tangent method. *Math. Comput. Appl.* **2018**, *23*, 35. [CrossRef]
20. Zahran, E.H.M.; Khater, M.M.A. Modified extended tanh-function method and its applications to the Bogoyavlenskii equation. *Appl. Math. Model.* **2016**, *40*, 1769–1775. [CrossRef]
21. Lv, S.; Wang, Z.; Chen, G. Modified extended tanh-function method to generalized nonlinear dispersive $mK(m, n)$ equation. *J. Math. Sci. Adv. Appl.* **2018**, *53*, 41–56. [CrossRef]
22. Suksamran, J.; Lenbury, Y.; Satiracoo, P.; Rattanakul, C. A model for porcine reproductive and respiratory syndrome with time-dependent infection rate: Traveling wave solution. *Adv. Differ. Equ.* **2017**, *215*, 1–11. [CrossRef]
23. Charpin, C.; Mahé, S.; Keranflec'h, A.; Belloc, C.; Cariolet, R.; Le Potier, M.-F.; Rose, N. Infectiousness of pigs infected by the porcine reproductive and respiratory syndrome virus (PRRSV) is time-dependent. *Vet. Res.* **2012**, *43*, 1–11. [CrossRef] [PubMed]
24. Keshet, L.E. *Mathematical Models in Biology*; Random House: New York, NY, USA, 2005.
25. Kuttler, C. Disease modelling and public health, part B. In *Handbook of Statistics*; Rao, A.S.R.S., Rao, S.P.C.R., Eds.; North Holland: Amsterdam, The Netherland, 2017; Volume 37, pp. 2–374.
26. Holton, G. Numerical solution, closed-form solution. In *Value-at-Risk: Theory and Practice*, 2nd ed.; Academic Press: Cambridge, MA, USA, 2013.